Pion Structure Function and Violation of the Momentum Sum Rule

J.P. Lansberg[1], F. Bissey, J.R. Cudell, J. Cugnon, M. Jaminon and P. Stassart

Université de Liège, Département de Physique B5, Sart Tilman,B-4000 LIEGE 1, Belgium

Abstract.
We present a method to evaluate the pion structure functions from a box diagram calculation. Pion and constituent quark fields are coupled through the simplest pseudoscalar coupling. The $\gamma^\star\pi \to q\bar{q}$ cross-section is evaluated and related to the structure functions. We then show that the introduction of non-perturbative effects, related to the pion size and preserving gauge invariance, provides us with a straighforward relation with the quark distribution. It is predicted that higher-twist terms become negligible for Q^2 larger than about 2 GeV^2 and that quarks in the pion have a momentum fraction smaller than in the proton. We enlarge the discussion concerning this violation of the momentum sum rule, emphasizing that the sum rule is recovered in the chiral limit and also when the finite size condition is not imposed.

1. INTRODUCTION

The usual way to describe quarks inside hadrons relies on the structure functions. Quantum Chromodynamics (QCD), being the theory of the interactions between quarks and gluons, is supposed to predict the structure functions, but in fact, these quantities result from non-perturbative effects and hence are not easily modeled. QCD is only able to predict their evolution as the virtuality of the probing photon (Q^2) changes. It is our purpose here to build a simple model for these quantities.

Phenomenological quark models, which possess some non-perturbative aspects and which are rather successful in reproducing low-energy properties of hadrons, are expected to help us understand the connection between deep-inelastic scattering (DIS) data and non-pertubative inputs. For very simple systems such as pions and other low-mass mesons, there exist some effective models (*e.g.* the Nambu-Jona-Lasinio (NJL) model) that incorporate, in some simplified way, special QCD features such as spontaneous chiral symmetry breaking and anomalies.

However, investigations of the structure functions along these lines have given rather different results [2, 3, 4]. This situation originates from the fact that the NJL model needs to be regularized and that different regularizations yield different results.

We present here an alternative way to evaluate of the pion structure function

[1] email: JPH.Lansberg@ulg.ac.be

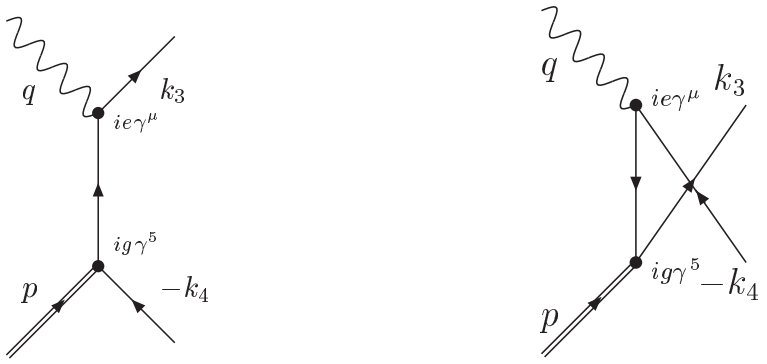

FIGURE 1. Feynman diagrams for the process $\gamma^\star\pi_0 \to q\bar{q}$.

based on Ref. [1], where the $q\overline{q}\pi$ vertex is represented by the simplest pseudoscalar coupling, *i.e.* $ig\gamma_5$ and the pion size is mimicked by the introduction of a gauge preserving cut-off.

2. CROSS-SECTION CALCULATION FOR $\gamma^\star\pi_0 \to Q\bar{Q}$ BY INTEGRATION OVER T

In this section, we calculate the cross-section for $\gamma^\star\pi_0 \to q\bar{q}$ which can be related to the form factors W_1 and W_2 as we shall see later. Another way to achieve this goal consists in calculating the imaginary part of the forward amplitude for $\gamma^\star\pi_0 \to \gamma^\star\pi_0$.

At the leading order in the loop expansion, we have the two diagrams shown in Fig. 1 which, when squared, give two types of contributions. The first one (corresponding to box-diagrams for the $\gamma^\star\pi_0 \to \gamma^\star\pi_0$ amplitude) enables us to calculate the structure functions straightforwardly. The second involves crossed quark lines and is related to processes where the two photons (in the $\gamma^\star\pi_0 \to \gamma^\star\pi_0$ scattering) are connected to different quark lines. This is incompatible with a probabilistic interpretation in terms of structure functions. As we will conclude from the calculations, contributions of this kind are fortunately higher-twists, *i.e.* they scale as $\frac{1}{Q^2}$, when we introduce the cut-off.

Their introduction is nevertheless mandatory, as this ensures gauge invariance (see Ref. [1]). This is required for a proper evaluation of the cross-section for the $\gamma^\star\pi_0 \to q\bar{q}$ process, which is a physical process, observable and thus gauge invariant.

2.1. Kinematics of the Process

For the sake of convenience, we work with cartesian coordinates in the CM (center of momentum) frame. The four-momenta of the four particles are given by:

$$q = (E(= q_0), \vec{q}), p = (E_\pi, -\vec{q}), k_3 = (k_{3,0}, \vec{k}_3), k_4 = (k_{4,0}, -\vec{k}_3). \tag{1}$$

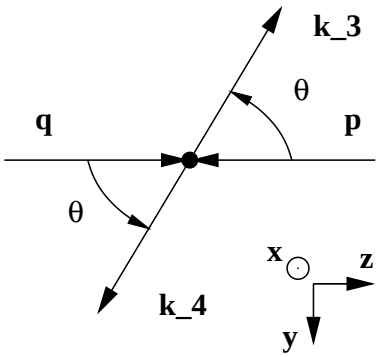

FIGURE 2. Kinematics and definition of the angle θ in the CM frame.

Let us now introduce the Mandelstam variables:

$$\begin{aligned} s &= (p+q)^2 = (k_3+k_4)^2 = E_{CM}^2 = (E+E_\pi)^2, \\ t &= (k_3-q)^2 = (k_4-p)^2, u = (k_3-p)^2 = (k_4-q)^2. \end{aligned} \tag{2}$$

We then define the square momenta:

$$q^2 = -Q^2, p^2 = m_\pi^2, k_3^2 = m^2, k_4^2 = m^2 \tag{3}$$

The variables of Eq. (1) can be written in terms of these quantities and of Mandelstam variables. One has:

$$k_{3,0} = k_{4,0} = \frac{\sqrt{s}}{2} \quad , \quad |\vec{k_3}| = |\vec{k_4}| = \sqrt{\frac{s}{4} - m^2}, \tag{4}$$

$$E \;=\; \frac{s - m_\pi^2 - Q^2}{2\sqrt{s}}, \tag{5}$$

and

$$|\vec{p}|^2 = |\vec{q}|^2 = E^2 + Q^2 = \frac{(s - m_\pi^2 - Q^2)^2 + 4sQ^2}{4s}. \tag{6}$$

The angle θ between the vectors $\vec{k}_3$ and $\vec{q}$ (see Fig. 2) is related to t by

$$t \;=\; m^2 + m_\pi^2 - s + \sqrt{s}\frac{s - m_\pi^2 - Q^2}{2\sqrt{s}} + 2\sqrt{\frac{s}{4} - m^2}\frac{\sqrt{(s - m_\pi^2 - Q^2)^2 + 4sQ^2}}{2\sqrt{s}}\cos\theta$$

Eventually we obtain:

$$\cos\theta = \frac{t - m^2 - \frac{m_\pi^2}{2} + \frac{s}{2} + \frac{Q^2}{2}}{2\sqrt{\frac{s}{4} - m^2}\frac{\sqrt{(s - m_\pi^2 - Q^2)^2 + 4sQ^2}}{2\sqrt{s}}} = \frac{t - m^2 - \frac{m_\pi^2}{2} + \frac{s}{2} + \frac{Q^2}{2}}{2\sqrt{\frac{s}{4} - m^2}\sqrt{E^2 + Q^2}}. \tag{7}$$

The physical values of t are lying between boundaries, corresponding to $\cos\theta = \pm 1$:

$$t_{\substack{\max\\\min}} = m^2 + \frac{m_\pi^2}{2} - \frac{s}{2} - \frac{Q^2}{2} \pm 2\sqrt{\frac{s}{4} - m^2}\frac{\sqrt{(s-m_\pi^2-Q^2)^2+4sQ^2}}{2\sqrt{s}} \tag{8}$$

Finally, assuming the incident direction along the z axis and the scattering in the $y-z$ plane, we get:

$$\begin{aligned}
q &= (\frac{s-m_\pi^2-Q^2}{2\sqrt{s}},0,0,\sqrt{\frac{(s-m_\pi^2-Q^2)^2+4sQ^2}{4s}}) = (E,0,0,\sqrt{E^2+Q^2}),\\
p &= (\sqrt{m_\pi^2+\frac{(s-m_\pi^2-Q^2)^2+4sQ^2}{4s}},0,0,-\sqrt{\frac{(s-m_\pi^2-Q^2)^2+4sQ^2}{4s}})\\
k_3 &= (\frac{\sqrt{s}}{2},0,-\sqrt{\frac{s}{4}-m^2}\sin(\theta),\sqrt{\frac{s}{4}-m^2}\cos\theta),\\
k_4 &= (\frac{\sqrt{s}}{2},0,\sqrt{\frac{s}{4}-m^2}\sin(\theta),-\sqrt{\frac{s}{4}-m^2}\cos\theta).
\end{aligned} \tag{9}$$

These quantities will be explicitly used in the determination of scalar products involving the polarisation vectors.

2.2. Amplitude Calculation

Applying Feynman rules for the processes shown in Fig. 1, we obtain the analytical expression of the square amplitude in a straightforward way. For a given polarisation of the virtual photon, $i = L, T_1, T_2$, and with well-known conventions[2] we have for the squared of the first diagram shown in Fig. 1,

$$\begin{aligned}
|\mathcal{M}_i|^2 = 3g^2(e_u^2+e_d^2)\mathrm{Tr}\Bigg(&(-\not{k}_4+m)\gamma^5\frac{\not{k}_3-\not{q}+m}{(k_3-q)^2-m^2}\gamma^{\mu'}\\
&(\not{k}_3+m)\gamma^\mu\frac{\not{k}_3-\not{q}+m}{(k_3-q)^2-m^2}\gamma^5\Bigg)\varepsilon_{i\mu}\varepsilon^\star_{i\mu'}.
\end{aligned} \tag{10}$$

The expression for the square of the second diagram as well as for the interference terms have similar expressions.

We first proceed to the calculation of the expressions of the scalar products of the polarisation vectors with q, p, k_3 and k_4 for the three possible polarisation states.

We shall use the following definition of the longitudinal polarisation vector,

$$\varepsilon_{L,\mu} = \frac{1}{\sqrt{Q^2}}(q_z,0,0,E). \tag{11}$$

---

[2] The isospin/charge factor $(e_u^2+e_d^2)$ corresponds to the following choice of the isospin matrix: $\pi^-: \begin{pmatrix}0&0\\\sqrt{2}&0\end{pmatrix}$ – $\pi^0: \begin{pmatrix}1&0\\0&-1\end{pmatrix}$ – $\pi^+: \begin{pmatrix}0&\sqrt{2}\\0&0\end{pmatrix}$ – $\gamma: \begin{pmatrix}e_u&0\\0&e_d\end{pmatrix}$

One has

$$\begin{aligned}
\varepsilon_L \cdot q &= 0, \\
\varepsilon_L \cdot p &= \frac{1}{\sqrt{Q^2}} \sqrt{s} \sqrt{E^2+Q^2}\ , \\
\varepsilon_L \cdot k_3 &= \frac{1}{\sqrt{Q^2}} \left(\frac{\sqrt{s}\sqrt{E^2+Q^2}}{2} - \frac{E(t-m^2-\frac{m_\pi^2}{2}+\frac{s}{2}+\frac{Q^2}{2})}{2\sqrt{E^2+Q^2}} \right).
\end{aligned} \tag{12}$$

For the linear transverse polarisation vectors, we use the following definition:

$$\varepsilon_{T_1,\mu} = (0,1,0,0),\ \varepsilon_{T_2,\mu} = (0,0,1,0). \tag{13}$$

This and Eq. (9) lead to:

$$\begin{aligned}
\varepsilon_{T_i} \cdot q &= 0 = \varepsilon_{T_i} \cdot p, \quad i=1,2, \\
\varepsilon_{T_1} \cdot k_3 &= 0, \\
\varepsilon_{T_2} \cdot k_3 &= \sqrt{\frac{s}{4}-m^2} \sqrt{1 - \left(\frac{t-m^2-\frac{m_\pi^2}{2}+\frac{s}{2}+\frac{Q^2}{2}}{2\sqrt{\frac{s}{4}-m^2}\sqrt{E^2+Q^2}} \right)^2}.
\end{aligned} \tag{14}$$

2.3. Polarised Cross-Sections

The total cross-section is given by the following relation [5], with $i = L, T_1, T_2$:

$$\frac{\mathrm{d}\sigma_i}{\mathrm{d}t} = \frac{1}{16\pi\lambda} \left| \mathcal{M}_i \right|^2 \tag{15}$$

with[3] $\lambda = \lambda(s, -Q^2, m_\pi^2)$. The latter directly links the amplitude –which is obtained, in our case, with REDUCE– and the cross-section differential upon t. Integrating over t from $t_{\min}$ to $t_{\max}$ (see Eq. (8)) gives the total cross-sections for given polarisations:

$$\sigma_i = \frac{1}{16\pi\lambda} 3g^2(e_u^2+e_d^2) \int \mathrm{d}t\ T^{\mu\mu'} \varepsilon_{i,\mu} \varepsilon^\star_{i\mu'}, \tag{16}$$

with $T^{\mu\mu'} \equiv \mathrm{Tr}\left((-\not{k}_4 + m)\gamma^5 \frac{\not{k}_3 - \not{q} + m}{(k_3-q)^2-m^2} \gamma^{\mu'} (\not{k}_3 + m) \gamma^\mu \frac{\not{k}_3 - \not{q} + m}{(k_3-q)^2-m^2} \gamma^5 \right)$.

It is also of interest to consider

$$\sigma_{contr.} = \frac{1}{16\pi\lambda} 3g^2(e_u^2+e_d^2) \int \mathrm{d}t\ T^{\mu\mu'} (g_{\mu\mu'} + \frac{q_\mu q_{\mu'}}{Q^2}) \tag{17}$$

since it does not involve any polarisation vectors and its calculation is somewhat easier. However, it should not confused with $\sigma_L + \sigma_{T_1} + \sigma_{T_2}$ (see later), which could be measured in some limiting experimental conditions.

---

[3] The function $\lambda(x,y,z)$ is defined as $\lambda(x,y,z) \equiv x^2+y^2+z^2-2xy-2xz-2yz$

2.4. The Cut-Off

2.4.1. Cut-off and Higher-twists

We introduce a cut-off in our calculations: instead of integrating over t from $t_{\min}$ to $t_{\max}$, we integrate from[4] $Max\{t_{\min}, \Lambda_t\}$ to $t_{\max}$. As shown in Ref. [1], this is equivalent to setting a cut-off for the square of the relative momentum of the quarks inside the pion, which can be considered as resulting from the finite size of the pion.

Irrespectively of the factors arising in the extraction of the structure functions (see section (3)), we can simply convince ourselves that in the presence of a cut-off the contribution of the crossed diagrams (the first photon hits a quark and the second an antiquark) are higher-twists, by plotting the ratio of these two contributions as a function of Q^2. The suppression is clear on Fig. 3 for whatever (finite) value of the cut-off; the curves are even indistinguishable in this case.

As we already said, in order to get a physical interpretation of our results –in terms of structure functions–, we need the crossed diagram contributions to be suppressed. The importance of a cut-off, which is not a regulator in the studied process, is thus manifest.

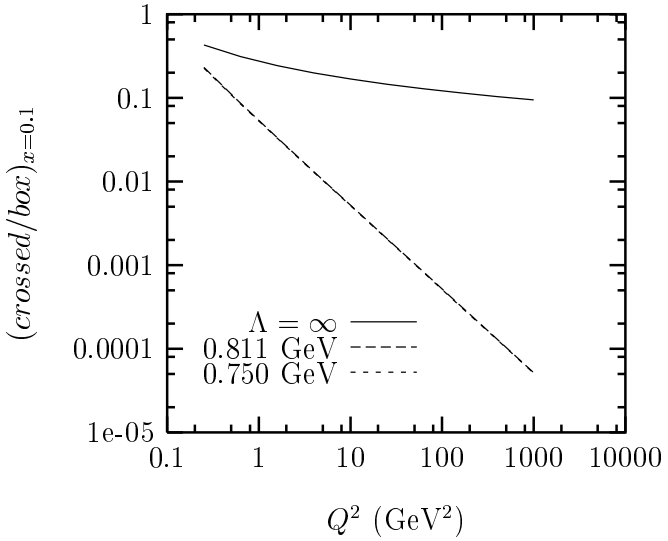

FIGURE 3. Ratio of the direct contributions to the crossed contributions to the cross-section for $\gamma^\star\pi^0 \to q\bar{q}$ at $x = 0.1$ and for three values of the cut-off Λ.

[4] Recall that $t < 0$.

2.4.2. Cut-off and Gauge Invariance

In most cases, the presence of a cut-off implies the breakdown of gauge invariance. This is the main reason why one commonly uses other regularization methods such as Pauli-Villars or dimensional regularization. In the context of an effective theory, a simple momentum cut-off has the critical advantage that the regularization parameter (which is kept to a finite value) can be interpreted as a physical one. In the case of dimensional regularization, the signification of fractional dimensional space is not at all clear. As for Pauli-Villars regularization, the introduction of wrong-sign fermionic contribution is not intuitive.

Nevertheless, in our model, as the intermediate states in $\gamma^\star\pi^0 \to \gamma^\star\pi^0$ are on-shell, the cut-off on the internal loop momentum[5] acts on a physical observable, that is t of the process $\gamma^\star\pi^0 \to q\bar{q}$. The conclusion is thus staightforward: this cut-off does not break gauge invariance.

This procedure would have been fully justified if we had only one pion vertex, and thus one condition to implement. But we have two vertices with two different expressions for the relative momenta. To keep gauge invariance, the cut-off on t must be on the overall cross-section as the physical observable is the full cross-section (the square of the sum of the two diagrams) at a given t.

To keep the constraint coming from the pion size, we should have imposed two conditions on the cross-section to be integrated over t. However, this would have given zero. As a makeshift we imposed one condition or the other.

Even if the physical interpretation is not so obvious, we thus kept gauge invariance, information from the pion size, suppressed the crossed diagrams and hence obtained an interpretation in terms of structure functions.

3. $\sigma_{\gamma^\star\pi_0\to Q\bar{Q}}$, W_1, W_2, F_1 AND F_2

At this stage we have calculated the polarised cross-sections and we should be able to link them to the structure functions for neutral pion. Before doing this, we shall first recall some mandatory formulae derived from the analysis of deep inelastic proton scattering.

We introduce the usual form of the hadronic tensor

$$W_{\mu\nu}(p,q) = (-g_{\mu\nu} - \frac{q_\mu q_\nu}{Q^2})W_1(Q^2,\nu) + [p_\mu + (\frac{p\cdot q}{Q^2})q_\mu][p_\nu + (\frac{p\cdot q}{Q^2})q_\nu]\frac{W_2(Q^2,\nu)}{M^2}, \quad (18)$$

with M, the hadron mass, and $W_1(Q^2,\nu)$ and $W_2(Q^2,\nu)$ the structure functions.

In the same spirit as for the definition of the cross-section of $\gamma^\star p \to X$ [6], we define the polarised cross-sections for $\gamma^\star\pi_0 \to X$ by [6]:

---

[5] which corresponds, up to some constants, to a cut-off on the relative mometum between the two quarks at the $\pi^0 q\bar{q}$ vertex.

[6] This definition is independent of the hadron spin because, on the one hand, we have to sum the contributions coming from the different polarisations and on the other hand, we have a spin

$$\sigma_i(\gamma^\star \pi_0 \to X) = \frac{4\pi^2\alpha}{K} \varepsilon_i^{\star\mu} \varepsilon_i^\nu W_{\mu\nu}, \tag{19}$$

with the flux factor $K = \frac{1}{2}\frac{\sqrt{\lambda(s,-Q^2,m_\pi^2)}}{m_\pi}$.

Defining the transverse cross-section through

$$\sigma_T \equiv \frac{1}{2}(\sigma_{T_1} + \sigma_{T_2}), \tag{20}$$

we can easily show that:

$$\begin{aligned} \sigma_T &= \frac{4\pi^2\alpha}{K} W_1, \\ \sigma_L &= \frac{4\pi^2\alpha}{K}\left[(1+\frac{\nu}{2xm_\pi^2})W_2 - W_1\right]. \end{aligned} \tag{21}$$

These last two formulae establish the link between the functions W_1 and W_2 and previously calculated polarised cross-sections for $\gamma^\star\pi_0 \to q\bar{q}$ (Eq. (16))[7].

---

factor arising in the relation between $W_{\mu\nu}$ and the hadronic current.

[7] Besides we would like to stress that one has to be cautious if one wants to consider non-polarised processes. Usually, a simple contraction of the amplitude for a given helicity with the expression,

$$-g^{\mu\nu} + \frac{q^\mu q^\nu}{M^2} \tag{22}$$

seems to be the most convenient way to proceed, instead of considering separately the different polarisations. This is in most cases licit because

$$\sum_{i=L,T_1,T_2} \varepsilon_i^{\star\mu}\varepsilon_i^\nu = -g^{\mu\nu} + \frac{q^\mu q^\nu}{M^2}, \tag{23}$$

for massive particles, and thus the –strict– sum over polarisations gives the *correct* tensor.

For spacelike virtual particles, nevertheless, we have the following normalisations

$$\begin{aligned} \varepsilon_T \cdot \varepsilon_T &= -1, \\ \varepsilon_L \cdot \varepsilon_L &= +1. \end{aligned} \tag{24}$$

Therefore, the following relation –which indeed reduces to Eq. (23) for massive particles for which Eq. (24) does not hold–,

$$\sum_i \frac{\varepsilon_i^{\star\mu}\varepsilon_i^\nu}{\varepsilon_i \cdot \varepsilon_i} = g^{\mu\nu} + \frac{q^\mu q^\nu}{Q^2} \tag{25}$$

leads, in this case, to

$$\sigma_{contr.} = \frac{4\pi^2\alpha}{K}\left(g^{\mu\nu} + \frac{q^\mu q^\nu}{Q^2}\right) W_{\mu\nu} = \sigma_L - 2\sigma_T \tag{26}$$

but not to $\sigma_L + 2\sigma_T$!

With all these tools, we can now extract the functions W_1 and W_2. Inverting for W_1 and W_2, we get

$$W_1 = \frac{\sqrt{\lambda}}{8\pi^2 m_\pi \alpha}\sigma_T \tag{27}$$

and

$$W_2 = \frac{\sqrt{\lambda}}{8\pi^2 m_\pi \alpha}\frac{2xm_\pi^2}{\nu + 2xm_\pi^2}(\sigma_L + \sigma_T). \tag{28}$$

We then get F_1 and F_2 through the usual scaling relations:

$$F_1(x) = MW_1(Q^2,\nu)\ , F_2(x) = \frac{\nu}{M}W_2(Q^2,\nu)\ , x = \frac{Q^2}{2p\cdot q} = \frac{Q^2}{2\nu}, \tag{29}$$

still with M for the hadron mass.

4. SUM RULES, PLOTS AND RESULTS

4.1. Number of Particles Sum Rule

The structure functions can now be related to the (valence) quark distributions:

$$F_1 = \frac{4}{18}(u_v(x) + \bar{u}_v(x)) + \frac{1}{18}(d_v(x) + \bar{d}_v(x)), \tag{30}$$

$$F_2 = 2xF_1. \tag{31}$$

We stress that the last relation, known as the Callan-Gross relation, comes out of our calculation. This does indicate that our approximations have been done consistently[8].

So far, we have only described the model. In order to make predictions, we need to fix its parameters, namely Λ, m and g. The latter can be thought of as the normalisation of the quark wave function, and we determine it by imposing that there are only two constituent quarks in the pion. In our model, the valence quark distributions are equal

$$u_v(x) = \bar{u}_v(x) = d_v(x) = \bar{d}_v(x) \equiv v(x). \tag{32}$$

The condition $\int_0^1 v(x)dx = 1/2$ then yields

$$\int_0^1 F_1(x)dx = \frac{5}{18}. \tag{33}$$

[8] For charged pions, the additional diagrams implying a direct coupling of the virtual photon to the pion are suppressed by a factor $1/s$ and the leading-twist results are the same, except for the charge coefficients entering Eq. (30) .

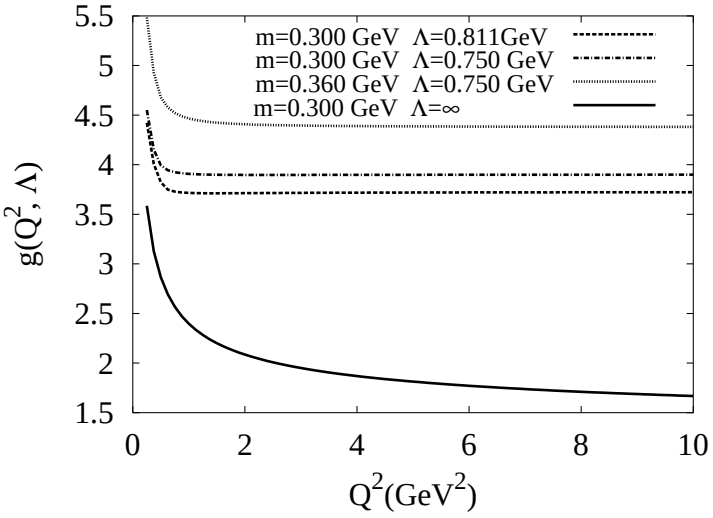

FIGURE 4. Values of the coupling constant $g(Q^2, \Lambda)$ which fulfill the sum rule (Eq. (33)), for the values of the parameters indicated at the top.

As F_1 is a function, not only of m and Λ, but also of Q^2, this gives us a coupling constant that evolves with Q^2. The resulting values of g are shown in Fig. 4 (right): for a finite cut-off Λ, the cross-section at fixed g would grow with energy, until the pion reaches its maximum allowed size, in which case the cross section would remain constant. If we impose relation Eq. (33), this means that $g(Q^2)$ will first decrease until the cut-off makes it reach a plateau for $Q^2 \gg \Lambda^2$ (in practice, the plateau is reached around $Q^2 \approx 2\Lambda^2$). The plateau value depends on m/Λ (and m_π/Λ).

4.2. Momentum Sum Rule

To constrain further our parameters, we can try to use the momentum sum rule

$$2\langle x \rangle = 4\int_0^1 xv(x)dx = \frac{18}{5}\int_0^1 F_2(x)dx. \tag{34}$$

In the parton model, this integral should be equal to 1 as $Q^2 \to \infty$, as we do not have gluons in the model.

Analyzing Fig. 5, it is clear that – at least for a finite value of Λ– the momentum sum rule is violated. For instance the momentum carried by the quarks at large Q^2 is 0.6 for $m = 300$ MeV and $\Lambda = 750$ MeV.

Nevertheless, there are two limits of our model that fulfill the condition $2\langle x \rangle = 1$ automatically and for which the quarks carry the entire momentum of the pion. First of all, if we do not impose that the pion has a finite size, then asymptotically we get $2\langle x \rangle$ =1. In the limit $m_\pi = 0$, we obtain the simple expression

$$2\langle x \rangle (\Lambda = \infty, m_\pi = 0) = \frac{4\ln(2\nu/m^2) - 3}{4\ln(2\nu/m^2) - 1}. \tag{35}$$

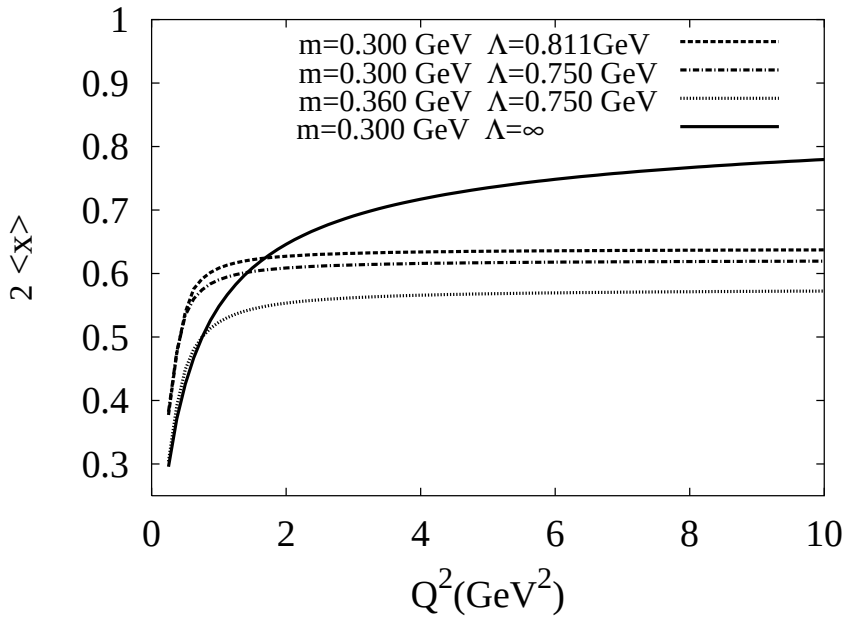

FIGURE 5. Momentum fraction of the quarks inside the neutral pion (Eq. 34), as a function of Q^2, for the values of the parameters indicated at the top of the figure.

This means that in that regime, for sufficiently high Q^2, the quarks behave as free particles, and the usual derivation based on the OPE holds [8].

The second case where this holds confirms this interpretation: if we impose $m \leq m_\pi/2$, the expressions we have given develop an infrared divergence, which corresponds to the case where both quarks emerging from the pion are on-shell and free. This divergence can be re-absorbed into the normalisation Eq. (33) of g, and the sum rule $2\langle x\rangle = 1$ is again automatically satisfied at large Q^2.

However, in the physical pion case, it makes more sense to consider that one of the quarks remains off-shell: the introduction of a cut-off changes the sum rule value, as the fields can never be considered as free. Hence, because of the Goldstone nature of the pion, one expects that the momentum sum rule will take a smaller value than in the case of other hadrons. This may explain why fits that assume the same momentum fraction for valence quarks in protons and pions [9] do not seem to leave any room for sea quarks [10].

We come back to the results for $2\langle x\rangle$ shown in Fig. 5. Again, the curves show a plateau at sufficiently large Q^2, with a value depending on m/Λ and m_π/Λ. It is easy to show that this value is always smaller than 1 as it can be guessed from Fig. 6.

Following the discussion in [1], we choose the following conservative values for the remaining parameters of our model: $m = 300$ MeV or 360 MeV and $\Lambda \simeq 800$ MeV.

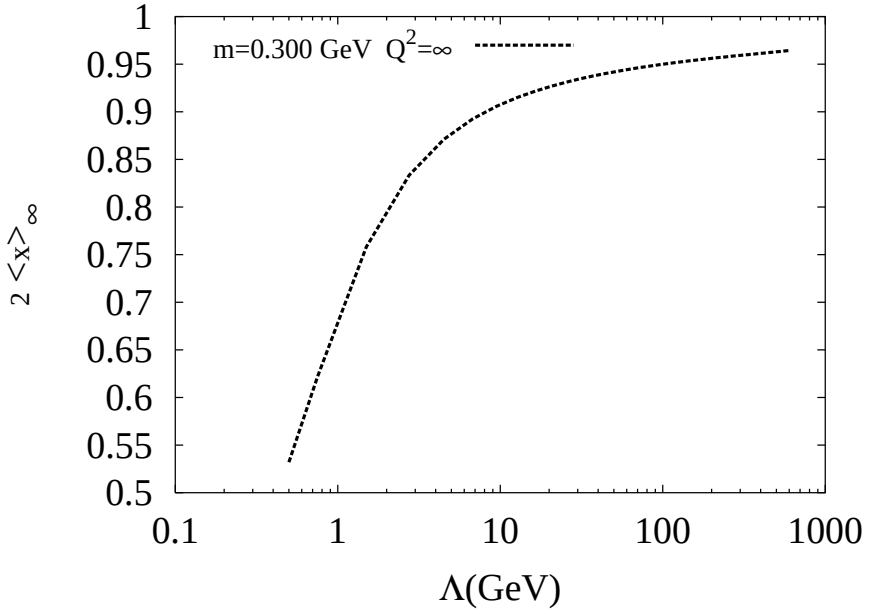

FIGURE 6. Asymptotic value (for large Q^2) of the momentum fraction of the quarks inside the neutral pion (Eq. 34), as a function of the cut-off Λ.

4.3. Plots of F_2

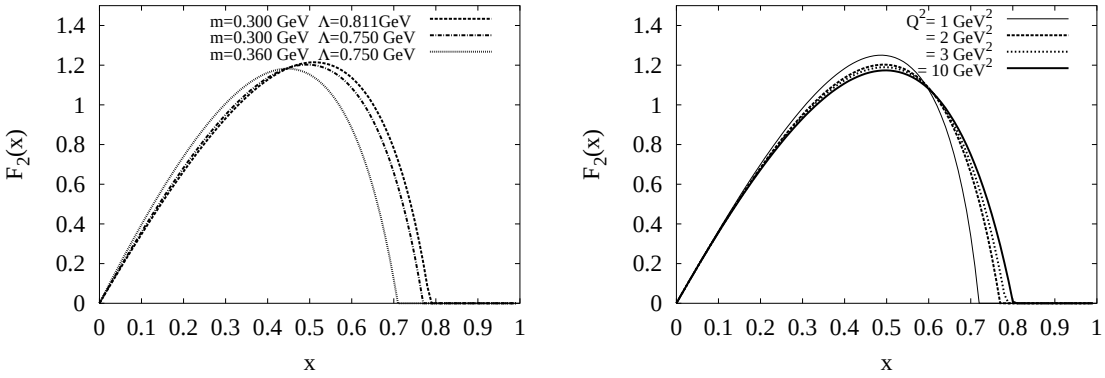

FIGURE 7. Structure function F_2 for the neutral pion. On the left, Q^2=2 GeV^2 and the values of the parameters m and Λ are as indicated. On the right, m=0.3 GeV and Λ=0.75 GeV and the values of Q^2 are as indicated.

Let us finally examine the properties of the distribution $v(x)$, or equivalently, of the function F_2. Some of our results are summarized in Fig. 7, for $Q^2 = 2$ GeV^2. The most striking feature is the vanishing of this function for x larger than some value x_{max}. This is again due to the fact that, because the quarks are not free in this model, the actual value of their mass does matter. It can clearly be seen that this effect originates from kinematical cuts (see Ref. [1]).

As a result, putting the cut quarks on-shell will be easier for small than for large x. Therefore, the x-distribution (F_1) is expected to be enhanced on the low x side, leading to a momentum fraction smaller than unity. The vanishing at large x is not obtained in similar works, in particular in the one of Ref. [2]. In this reference, the Bjorken limit is taken first and the kinematical constraint is not applied. This procedure seems questionable for evaluating cross-sections at finite Q^2.

5. CONCLUSION

We have discussed the simplest model allowing to relate $\gamma^\star\pi \to q\bar{q}$ to the pion quark distributions. The model consists in calculating the simplest diagrams for a γ^5 coupling between pion and constituent quark fields.

We show that the crossed diagrams, which are to be included in order to guarantee gauge invariance, preclude the existence of the relation between the the cross-section and the quark distribution. The introduction of a cut-off on t allows such a relation without breaking gauge invariance. The cut-off on t being equivalent to a cut-off on the square of the relative momentum of the quarks inside pion, this effect can be traced back to the finite size of the pion. For reasonable value of the cut-off, the crossed diagrams become negligible as soon as Q^2 is larger than 2 GeV^2 allowing quark distributions to be meaningful even for relatively small Q^2.

One of the most important outcomes of our calculation is the deviation from the momentum sum rule. However, we recover this sum rule ($2\langle x\rangle = 1$) in two limiting cases, which correspond to free quarks. The first one is the limit $\Lambda \to \infty$. The second one is for $m < \frac{m_\pi}{2}$. Then, an infrared divergence appears, which can be reabsorbed into the normalisation of g and the momentum sum rule is again recovered for large Q^2. Hence, the violation of the sum rule can tentatively be attributed to the Goldstone boson nature of the pion.

ACKNOWLEDGMENTS

This work has been performed in the frame of ESOP Collaboration and has benefited from the financial support of the EU (contract N° HPRN-CT-2000-00130).

REFERENCES

1. F. Bissey, J. R. Cudell, J. Cugnon, M. Jaminon, J. P. Lansberg and P. Stassart, Phys. Lett. B **547**, 210 (2002) [arXiv:hep-ph/0207107].
2. T. Shigetani, K. Suzuki and H. Toki, Phys. Lett. B **308**, 383 (1993) [arXiv:hep-ph/9402286].
3. R. M. Davidson and E. Ruiz Arriola, Phys. Lett. B **348**, 163 (1995) ; H. Weigel, E. Ruiz Arriola and L. P. Gamberg, Nucl. Phys. B **560**, 383 (1999) [arXiv:hep-ph/9905329].
4. R. M. Davidson and E. Ruiz Arriola, Acta Phys. Polon. B **33**, 1791 (2002) [arXiv:hep-ph/0110291].
5. V.D. Barger and R.J.N. Philips, *Collider Physics*, Addison-Wesley, Menlo Park, 1987.
6. I.J.R. Aitchison and A.J.G. Hey, *Gauge Theories in Particles Physics* (first edition), Institute of Physics Publishing, Bristol, 1982, p. 95.
7. C. G. Callan and D. J. Gross, *Phys. Rev. Lett.* **22**, 156 (1969).
8. C. Itzykson and J. B. Zuber, *Quantum Field Theory*, New York, U.S.A.: McGraw-Hill (1980) 705 P. (International Series In Pure and Applied Physics).
9. M. Glück, E. Reya and I. Schienbein, Eur. Phys. J. C **10**, 313 (1999) [arXiv:hep-ph/9903288].
10. M. Klasen, J. Phys. G **28**, 1091 (2002) [arXiv:hep-ph/0107011].